[DOI]10.12016/j.issn.2096-1456.2022.06.003

·基础研究·

钛表面不同硅烷偶联c(RGDfK)环肽的表征及生物相容性分析

周齐悦[1]，　洪高英[1]，　吴桐[1]，　陈晨[2]，　谢海峰[1]
1. 南京医科大学附属口腔医院修复科 江苏省口腔疾病研究重点实验室 江苏省口腔医学转化医学工程研究中心，江苏 南京(210029)；　2. 南京医科大学附属口腔医院牙体牙髓科 江苏省口腔疾病研究重点实验室 江苏省口腔医学转化医学工程研究中心，江苏 南京(210029)

【摘要】　目的　探讨用四种不同硅烷将c(RGDfK)[(cyclo(Arg-Gly-Asp-d-Phe-Lys)]环肽固定于钛表面的效率及生物相容性。**方法**　钛表面经碱热处理(OH组)，分别用3-氨丙基三乙氧基硅烷(3-aminopropyltriethoxysilane，APTES)(OHAP组)、3-氯丙基三乙氧基硅烷(3-chloropropyltriethoxysilane，CPTES)(OHCP组)、3-巯基丙基三甲氧基硅烷(3-mercaptopropyltriethoxysilane，MPTS)(OHMPT组)、3-异丁烯酰氧丙基三甲氧基硅烷(γ-methacryloxypropyltrimethoxysilane，γ-MPS)(OHMPS组)四种硅烷固定c(RGDfK)环肽，构建钛-硅烷-c(RGDfK)环肽涂层，钛片表面未处理组为空白对照组(NT组)。利用扫描电镜、接触角计观察各组涂层表面形貌及润湿性变化，通过X射线光电子能谱分析钛表面元素组成，4，6-二氨基-2-苯基吲哚(4，6-diamino-2-phenylindole，DAPI)与鬼笔环肽荧光染色后使用激光共聚焦显微镜观察材料表面小鼠前成骨细胞MC3T3-E1黏附情况，细胞计数(cell counting kit-8，CCK-8)试验和碱性磷酸酶(alkaline phosphatase，ALP)活性测定评价材料表面MC3T3-E1细胞增殖及成骨分化情况。**结果**　扫描电镜观察可见碱热处理后钛表面形成海绵状三维立体网状结构，硅烷-c(RGDfK)环肽涂层附着其上，各组润湿性较未处理钛片均有较大提高，OHMPS组Si/Ti、酰胺-N/Ti元素比最高；OHAP组细胞黏附形态最佳；OHAP组、OHMPT组、OHMPS组细胞增殖及ALP活性均显著高于对照组($P < 0.05$)；OHCP组细胞增殖活性及ALP活性与对照组无统计学差异。**结论**　MPTS、CPTES、γ-MPS三种硅烷均能够作为偶联剂将c(RGDfK)环肽结合于钛表面，促进MC3T3-E1细胞黏附、增殖和分化，其中γ-MPS偶联c(RGDfK)环肽的效果最好，而MPTS、CPTES、γ-MPS偶联c(RGDfK)环肽后具有相似的生物学性能。

【关键词】　钛种植体；　c(RGDfK)；　硅烷偶联剂；　碱热处理；　表面处理；　MC3T3-E1细胞；　细胞黏附；　成骨分化；　碱性磷酸酶
【中图分类号】　R78　**【文献标志码】**　A　**【文章编号】**　2096-1456(2022)06-0398-08
【引用著录格式】　周齐悦，洪高英，吴桐，等. 钛表面不同硅烷偶联c(RGDfK)环肽的表征及生物相容性分析[J]. 口腔疾病防治，2022，30(6)：398-405. doi：10.12016/j.issn.2096-1456.2022.06.003.

微信公众号

Characterization and biocompatibility analysis of different silanes coupling c(RGDfK) cyclic peptide on titanium surfaces

ZHOU Qiyue[1], HONG Gaoying[1], WU Tong[1], CHEN Chen[2], XIE Haifeng[1]. 1. Department of Prosthodontics, Affiliated Stomatology Hospital of Nanjing Medical University, Jiangsu Province Key Laboratory of Oral Diseases, Jiangsu Province Engineering Research Center of Stomatological Translational Medicine, Nanjing 210029, China; 2. Department of Endodontics, Affiliated Stomatology Hospital of Nanjing Medical University, Jiangsu Province Key Laboratory of Oral Diseases, Jiangsu Province Engineering Research Center of Stomatological Translational Medicine, Nanjing 210029, China
Corresponding author: XIE Haifeng, Email: xhf-1980@126.com, Tel: 86-25-69593081

【收稿日期】2021-09-01；　**【修回日期】**2021-11-11
【基金项目】国家自然科学基金项目(81970927)；江苏省卫生健康委科学技术基金项目(M2020066)；江苏高校优势学科建设工程资助项目(2018-87)
【作者简介】周齐悦，硕士研究生，Email：2531960376@qq.com
【通信作者】谢海峰，主任医师，博士，Email：xhf-1980@126.com，Tel：86-25-69593081

【**Abstract**】 **Objective** To compare the efficiency and biocompatibility of four different silanes on immobilizing c(RGDfK) peptide on titanium surface. **Methods** After alkali-heat treatment (group OH), the titanium surface was treated with 3-aminopropyltriethoxysilane (APTES) (group OHAP), 3-chloropropyltriethoxysilane (CPTES) (group OHCP) (3-mercaptopropyltrimethoxysilane (MPTS) (group OHMPT) and 3-isobutyryloxy propyltrimethoxysilane(γ- MPS) (group OHMPS) to immobilize the c(RGDfK) cyclic peptide and constructa titanium-silane-c(RGDfK) coating. The NT group was the blank control group. The surface morphology and wettability of the coatings were detected using scanning electron microscopy and contact angle measurement. The elemental composition of the titanium surface was analyzed using X-ray photoelectron spectroscopy. After fluorescent staining with 4',6-diamino-2-phenylindole (DAPI) and phalloidin, the adhesion of mouse preosteoblast MC3T3-E1 cells on the surface of the materials was observed using laser confocal microscopy. Cell counting kit-8 (CCK-8) and alkaline phosphatase (ALP) activity assays were used to evaluate the proliferation and osteogenic differentiation of MC3T3-E1 cells on the surface of the materials, respectively. **Results** Scanning electron microscope observation showed a spongy-like 3-dimensional network formed on the titanium surface after alkali-heat treatment with silane-c(RGDfK) coating adhesion. The wettability of each group was greatly improved compared to the untreated titanium surface. The element ratios of Si/Ti and amide-N/Ti in the OHMPS group were the highest. The OHAP group exhibited the best cell adhesion effect. The cell proliferation and ALP activity of the OHAP, OHMPT, and OHMPS groups were significantly higher than the control group ($P < 0.05$); there was no statistical difference between the OHCP group and the control group. **Conclusion** MPTS, CPTES and γ-MPS covalently immobilized cyclic peptide c(RGDfK) on the titanium surface, which promoted adhesion, proliferation and osteogenic differentiation of MC3T3-E1 cells. Theγ-MPS conjugated C (RGDfK)cyclic peptide exhibited the best effect. MPTS, CPTES and γ-MPS coupled with c(RGDfK) cyclic peptides had similar biological properties.

【**Key words**】 titanium implants; c(RGDfK); silane coupling agent; alkali-heat treatment; surface treatment; MC3T3-E1; cell adhesion; osteogenic differentiation; ALP

J Prev Treat Stomatol Dis, 2022, 30(6): 398-405.

【**Competing interests**】 The authors declare no competing interests.

This study was supported by the grants from National Natural Science Foundation of China (No. 81970927); Medical Research Projects of the Health Department of Jiangsu Province (No. M2020066); Priority Academic Program Development of Jiangsu Higher Education Institutions (No. 2018-87).

钛的骨结合能力与表面结构和化学组成密切相关，对钛金属进行表面处理及负载涂层，可改变钛表面的微观结构和化学组成，从而提高细胞早期黏附和成骨分化水平[1-2]。精氨酸-甘氨酸-天冬氨酸（Arg-Gly-Asp，RGD）多肽是一种有效且常用的刺激细胞黏附的肽序列，被发现能促进成骨细胞的生长，促使骨组织再生[3]。以往研究中，学者以硅烷偶联的方式形成了钛-硅烷-RGD多肽的三层结构，证实可以促进细胞黏附、增殖以及成骨分化[4-6]。硅烷种类繁多，尤其是末端基团的不同可能给硅烷提供不同的化学活性，然而尚未见研究对比钛表面以不同末端基团的硅烷偶联RGD多肽的效率及所实现的细胞活性。本研究使用氨基、巯基、氯基、烯酰氧基4种不同末端的硅烷，即3-氨丙基三乙氧基硅烷（3-aminopropyltriethoxysilane，APTES）、3-氯丙基三乙氧基硅烷（3-chloropro-pyltriethoxysilane，CPTES）、3-巯基丙基三甲氧基硅烷（3-mercaptopropyltriethoxysilane，MPTS）、3-异丁烯酰氧丙基三甲氧基硅烷（γ-methacryloxypropyltrimethoxysilane，γ-MPS）作为偶联剂将c(RGDfK)环肽固定于钛表面，对各组的化学结合进行表征分析，并对比其对MC3T3-E1细胞黏附、增殖及分化的影响。

1　材料和方法

1.1　主要材料与试剂

小鼠前成骨细胞MC3T3-E1细胞（中国科学院细胞库，中国），钛片（陕西盛辉钛业有限公司，中国），APTES、CPTES、MPTS、γ-MPS（麦克林，中国），c(RGDfK)（合肥国肽生物科技有限公司，中国），磷酸缓冲盐溶液（phosphate buffered saline，PBS）（白鲨，中国），胎牛血清（Cell Sciences，美国），青霉素/链霉素溶液（Gibco，美国），α-MEM（α-minimum essential medium，α-MEM）培养基（Gibco，美国），4',

6-二氨基-2-苯基吲哚(4,6-diamino-2-phenyl indole,DAPI)(Apexbio,美国),鬼笔环肽(Apexbio,美国),CCK-8试剂盒(Dojindo Molecular Technology,Kumamoto,日本),碱性磷酸酶(alkaline phosphatase,ALP)检测试剂盒(南京建成,中国),BCA(Bicinchoninic acid,BCA)蛋白质浓度测定试剂盒(碧云天,中国),接触角计(SL250,Kino Industry,Boston,MA,美国),X射线光电子能谱(X-ray photoelectron spectroscopy,XPS)(Escalab 250xi,Thermo Fisher Scientific,美国),扫描电镜(scanning electron microscope,SEM)(MAIA3 TESCAN,捷克),激光共聚焦扫描显微镜(confocal laser scanning microscope,CLSM)(LSM 780,CalZeiss AG,德国),酶标仪(PerkinElmer,Waltham,MA,美国)。

1.2　涂层制备方法

加工24枚直径30 mm、厚1 mm的圆形钛片以及48枚直径5 mm、厚1 mm的圆形钛片。所有钛片用400目、800目、1 200目、2 000目研磨用碳化硅纸依次进行机械抛光。抛光后,用丙酮、乙醇和超纯水依次超声清洗15 min,60 ℃烘干后置于干燥皿中保持干燥。

钛片分组处理(直径30 mm钛片每组4个,直径5 mm钛片每组8个):① NT组,钛片表面不做处理,空白对照组;② OH组,碱热处理,即10 mL 60 ℃的5 mol/L NaOH溶液中浸泡24 h,超纯水冲洗两遍,37 ℃干燥[7];③ OHAP组,碱热处理后,在50 mL 5%APTES的无水乙醇溶液中常温避光浸泡24 h,随后取出,无水乙醇中超声清洗15 min以去除物理吸附的硅烷颗粒,37 ℃干燥,在110 ℃下固化1 h[4-5];④ OHCP组,碱热处理,使用CPTES与OHAP组同法做硅烷化处理;⑤ OHMPT组,碱热处理,使用MPTS与OHAP组同法做硅烷化处理,硅烷处理后在1%戊二醛溶液中浸泡1 h,超纯水冲洗,37 ℃干燥;⑥ OHMPS组,碱热处理,使用γ-MPS与OHAP组同法做硅烷化处理。上述OHAP、OHCP、OHMPT、OHMPS组钛片分别处理后,高压蒸汽灭菌,然后浸入4 ℃的0.1 mg/mL c(RGDfK)肽/PBS溶液中15 h,取出后PBS清洗,常温干燥。细胞培养之前,所有样本均紫外消毒,并用PBS冲洗。

1.3　表面处理的表征分析

1.3.1　表面润湿性能　各组随机选取直径30 mm钛片1枚,以1 μL去离子水为检测液,使用接触角计测量中心点的接触角。

1.3.2　X射线光电子能谱(XPS)分析　随机选取直径5 mm钛片1枚,XPS评估表面硅烷化及c(RGDfK)连接情况。在225 W下用单色AlKa辐照(1 486.7 eV)进行测量,入射角为90°。使用XPSPEAK41软件进行光谱分析,评估Si2p、Cl2p、C1s、N1s、titanium2p、O1s的强度。

1.3.3　表面形貌　每组挑选1枚直径5 mm钛片喷金,SEM在二次电子模式下观察,工作电压20 kV,工作距离(5.425 ± 0.5)mm。

1.4　细胞行为

1.4.1　细胞培养　将小鼠前成骨细胞MC3T3-E1细胞在添加10%胎牛血清和1%青霉素/链霉素溶液的α-MEM培养基中,置于37 ℃含5% CO_2的培养箱中培养。检测ALP活性时,细胞在添加50 μg/mL抗坏血酸、10 Mm β-甘油磷酸盐和10nM地塞米松的上述培养基中孵育以诱导成骨分化。

1.4.2　细胞黏附试验　将直径为5 mm的钛片样品置于96孔板中,每组1个,以3 000个/孔的密度接种细胞。培养6 h后,将黏附在钛片表面的细胞用4%多聚甲醛固定20 min,然后在室温下用0.5% Triton X-100在PBS中通透15 min,用DAPI对细胞核进行染色,用鬼笔环肽对细胞骨架进行染色。使用CLSM观察细胞形态。

1.4.3　细胞增殖试验　将直径为5 mm的钛片样品置于96孔板中,每组5个,以3 000个/孔的密度接种细胞。培养7 d后使用CCK-8试剂盒检测细胞增殖率。使用酶标仪测量450 nm处的吸光度值。以含有CCK-8溶液但没有接种细胞的孔为空白对照。

增殖率(%)=(各实验组吸光度平均值−空白孔吸光度平均值)/(无材料只有细胞组吸光度平均值−空白孔吸光度平均值)× 100%

1.4.4　ALP活性检测　将直径为30 mm的钛片样品置于6孔板中,每组3个,以8×10^5个/孔的密度接种细胞,7 d后,使用ALP检测试剂盒检测ALP活性,并使用BCA蛋白质浓度测定试剂盒检测的蛋白总量作为标准。

1.5　统计学分析

使用SPSS 22,对上述接触角测量、细胞增殖、ALP活性检测实验数据进行分析,在方差齐性条件下采用单因素方差分析和LSD-t检验来评估组间差异,以$P < 0.05$为差异具有统计学意义。

2　结　果

2.1　处理表面的表征分析

SEM观察显示,抛光的钛片呈光滑表面,碱热

处理在钛片表面形成了海绵状三维立体网状结构，孔径大小约为100～200 nm，接枝各种硅烷及c(RGDfK)环肽使部分孔隙被填满(图1)。

接触角测量结果显示，抛光的钛片接触角超过90°，提示并非亲水性表面；碱热处理后的多孔结构使接触角急剧降低，呈现极亲水的状态；而进一步接枝硅烷及多肽后，各组水接触角则均有不同程度的回升，其中OHMPS组的接触角回升最多($F = 0.142$；OHAP组：$P < 0.05$；OHCP组：$P < 0.05$；OHMPT组：$P < 0.05$；OHMPS组：$P < 0.05$)(图2)。

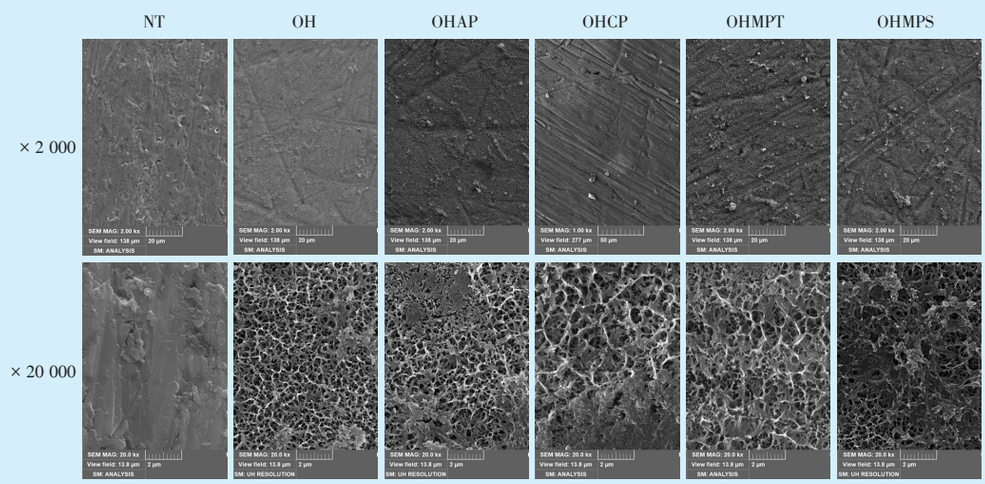

The specimens were sprayed with gold, and the surface morphology was observed using SEM. Group NT has a smooth surface, and a spongy three-dimensional network structure is formed in group OH after alkali-heat treatment. Some of the pores are filled by grafting different silanes and c (RGDfK) cyclic peptides in the OHAP, OHCP, OHMPT and OHMPS groups. Group NT: untreated; group OH: alkali-heat-treatment; group OHAP: APTES coupling; group OHCP: CPTES coupling; group OHMPT: MPTS coupling; group OHMPS: γ-MPS coupling. APTES: 3-aminopropyltriethoxysilane; CPTES: 3-chloropropyltriethoxysilane; MPTS: 3-mercaptopropyltriethoxysilane; γ-MPS: γ-methacryloxypropyltrimethoxysilane; SEM: scanning electron microscope

Figure 1　SEM micrographs of different silanes coupling c(RGDfK) on titanium surfaces

图1　钛表面不同硅烷偶联c(RGDfK)环肽的表面形貌SEM图像

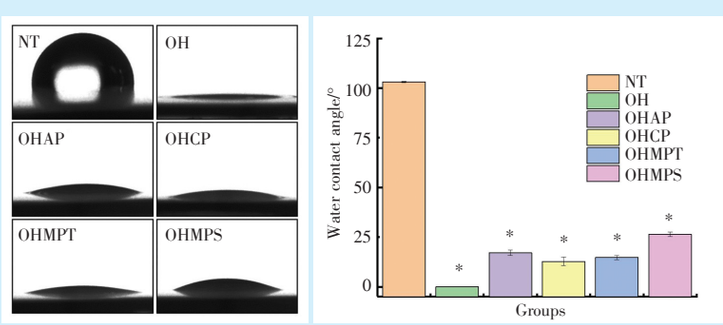

The contact angle of the NT group was greater than 90° but decreased to 0° after alkali-heat treatment. After further grafting with silane and polypeptides, the water contact angle increased to different degrees in each group.*: compared with NT group, $P < 0.05$. Group NT: untreated; group OH: alkali-heat-treatment; group OHAP: APTES coupling; group OHCP: CPTES coupling; group OHMPT: MPTS coupling; group OHMPS: γ-MPS coupling. APTES: 3-aminopropyl triethoxysilane; CPTES: 3-chloropropyltriethoxysilane; MPTS: 3-mercaptopropyl triethoxysilane; γ-MPS: γ-methacryloxypropyltrimethoxysilane; SEM: scanning electron microscope

Figure 2　Surface wettability changes of different silanes coupling c(RGDfK) on titanium surfaces

图2　钛表面不同硅烷偶联c(RGDfK)环肽表面润湿性变化

XPS结果显示，碱热处理后钛表面O元素增加，证明活化后大量羟基成功负载于钛表面，负载硅烷及c(RGDfK)环肽后Si、N元素含量增加，提示硅烷及多肽的有效连接(表1)。Si/Ti值结果提示

OHMPS组硅烷的负载量相对于其他三种硅烷高数倍，提示γ-MPS与活化后钛表面的结合能力最强。

OHAP、OHCP、OHMPS组N元素峰呈现出两种组分，为399.8～400.2 eV及401～402 eV，分别对应蛋白质中酰胺键和伯胺[4]，各组中酰胺键的含量为83%～88%，而OHMPT组N元素中均为酰胺键成分（图3）。

根据酰胺-N/Ti元素比，OHMPS组负载c

表1　XPS分析表面元素含量

Table 1　XPS analysis of surface element content

Groups	C(%)	N(%)	O(%)	Si(%)	Ti(%)	BAL(%)	Amide-N/Ti	Si/Ti
NT	54.62	1.50	35.32	0.83	7.72	0.01		
OH	25.52	0.33	52.62	0.50	21.03	0.00		
OHAP	26.58	0.67	54.27	0.75	16.94	0.79	0.035	0.04
OHCP	26.72	1.01	51.67	1.02	17.56	2.02	0.048	0.06
OHMPT	26.54	0.95	52.95	1.10	16.97	1.49	0.056	0.06
OHMPS	31.97	0.88	44.49	3.31	12.58	6.77	0.062	0.26

Group NT: untreated; group OH: alkali-heat-treatment; group OHAP: APTES coupling; group OHCP: CPTES coupling; group OHMPT: MPTS coupling; group OHMPS: γ-MPS coupling. APTES: 3-aminopropyltriethoxysilane; CPTES: 3-chloropropyltriethoxysilane; MPTS: 3-mercaptopropyl triethoxysilane; γ-MPS: γ-methacryloxypropyltrimethoxysilane; BAL: balance, remaining content; XPS: X ray photoelectron spectroscopy

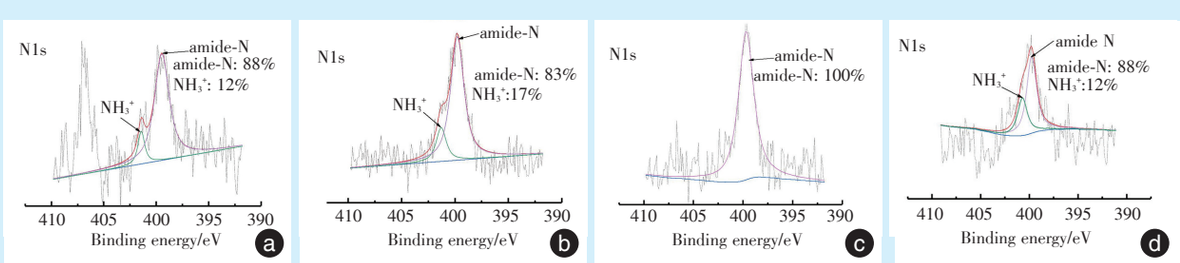

a: APTES coupling (group OHAP); b: CPTES coupling (group OHCP); c: MPTS coupling (group OHMPT); d: γ-MPS coupling (group OHMPS). Group OHAP: APTES coupling; group OHCP: CPTES coupling; group OHMPT: MPTS coupling; group OHMPS: γ-MPS coupling. APTES: 3-aminopropyl triethoxysilane; CPTES: 3-chloropropyltriethoxysilane; MPTS: 3-mercaptopropyltriethoxysilane; γ-MPS: γ-methacryloxypropyltrimethoxysilane; XPS: X-ray photoelectron spectroscopy

Figure 3　XPS peaks of N1s of different silanes coupling c(RGDfK) on titanium surfaces in groups

图3　钛表面不同硅烷偶联c（RGDfK）环肽各组XPS中N1s峰谱图

（RGD）fK环肽稍高于OHCP组及OHMPT组，但远未达到该组硅烷负载率的优势，OHAP组结合的c（RGD）fK含量最少。

2.2　细胞黏附性比较

激光共聚焦扫描显微镜观察6组钛试件与MC3T3-E1细胞共培养6 h后的细胞黏附情况（图4），可见NT组细胞铺展不佳，呈长梭形，未观察到明显的细胞伪足。OH组、OHAP组、OHCP组、OHMPT组、OHMPS组细胞铺展呈圆形，见较多细胞微丝；其中，OHAP组的钛片细胞铺展最好，伪足伸展最为充分。

2.3　细胞增殖情况比较

MC3T3-E1细胞与钛试件共培养7 d后，OHAP、OHMPT、OHMPS组均显示出良好的增殖潜力，与NT组相比有显著差异（$F=0.089$；OHAP组：$P=0.013$；OHMPT组：$P=0.002$；OHMPS组：$P=0.025$）（图5）。OHMPT组增殖活性最好。OH组和OHCP组与NT组相比，差异无统计学意义（OH组：$P=0.934$；OHCP组：$P=0.139$）。

2.4　细胞成骨活性比较

各组钛片表面接种MC3T3-E1细胞并进行成骨诱导7 d的ALP活性如图6所示，可以发现各种硅烷-c（RGDfK）环肽处理组均促进了细胞ALP的表达，其中，OHAP、OHMPT、OHMPS组的相对表达量较高，与NT组相比差异有统计学意义（$F=0.051$，OHAP组：$P=0.002$；OHMPT组：$P=0.007$；

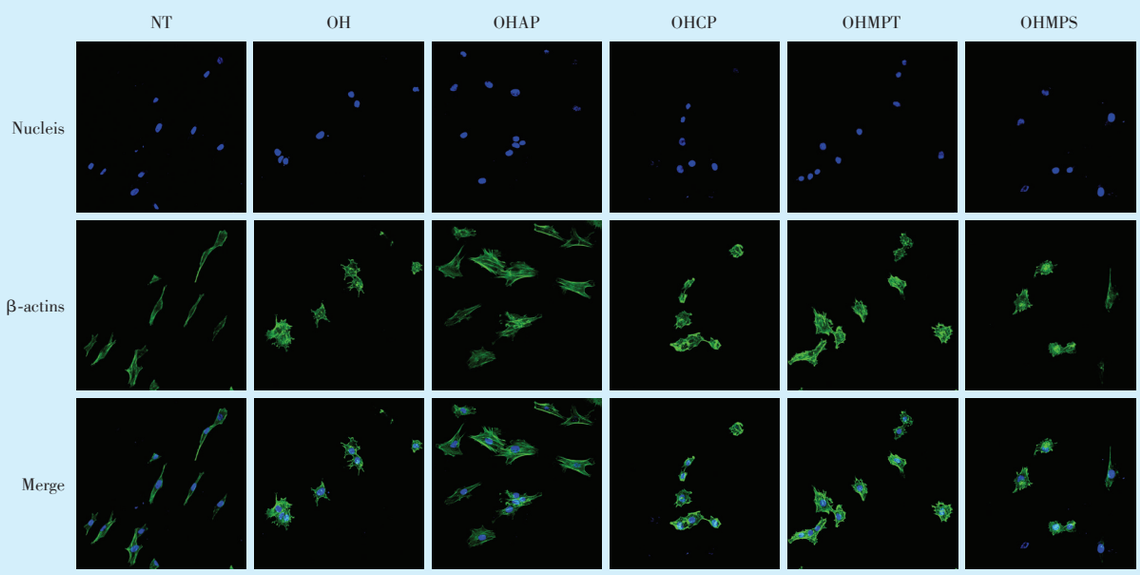

Immunofluorescence staining of β-actin (green) and nuclei (blue) in MC3T3-E1 cells 6 h after seeding on titanium samples. Cells in the NT group were not well spread and were long spindle shaped with no obvious pseudopodia. Cells in the OH, OHAP, OHCP, OHMPT and OHMPS groups were circular in shape, and more cell microfilaments were observed. Original magnification is × 200. Group NT: untreated; group OH: alkali-heat-treatment; group OHAP: APTES coupling; group OHCP: CPTES coupling; group OHMPT: MPTS coupling; group OHMPS: γ-MPS coupling. APTES: 3-aminopropyl triethoxysilane; CPTES: 3-chloropropyltriethoxysilane; MPTS: 3-mercaptopropyl triethoxysilane; γ-MPS: γ-methacryloxypropyl trimethoxysilane

Figure 4　Cell adhesion of different silanes coupling c(RGDfK) on titanium surfaces was observed using confocal laser scanning microscope

图4　激光共聚焦扫描显微镜观察钛表面不同硅烷偶联c(RGDfK)环肽各组细胞黏附情况

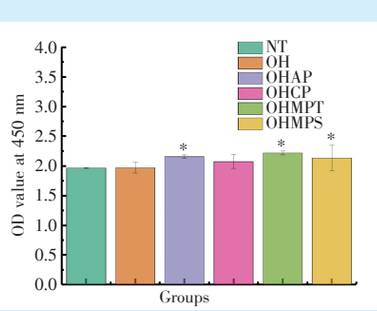

*: compared with NT group, $P < 0.05$, $n = 5$. Group NT: untreated; group OH: alkali-heat-treatment; group OHAP: APTES coupling; group OHCP: CPTES coupling; group OHMPT: MPTS coupling; group OHMPS: γ-MPS coupling. APTES: 3-aminopropyl triethoxysilane; CPTES: 3-chloropropyl triethoxysilane; MPTS: 3-mercaptopropyltriethoxysilane; γ-MPS: γ-methacryloxypropyl trimethoxysilane

Figure 5　Cell proliferation of different silanes coupling c(RGDfK) on titanium surfaces was detected using CCK-8 assay

图5　CCK-8法检测钛表面不同硅烷偶联c(RGDfK)环肽各组细胞增殖活性

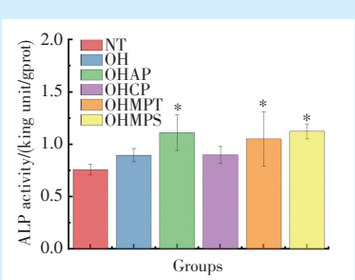

*: compared with NT group, $P < 0.05$. Group NT: untreated; group OH: alkali-heat-treatment; group OHAP: APTES coupling; group OHCP: CPTES coupling; group OHMPT: MPTS coupling; group OHMPS: γ-MPS coupling. APTES: 3-aminopropyl triethoxysilane; CPTES: 3-chloropropyl-triethoxysilane; MPTS: 3-mercaptopropyltriethoxysilane; γ-MPS: γ-methacryloxypropyltrimethoxysilane; ALP: alkaline phosphatase

Figure 6　ALP activity of different silanes coupling c(RGDfK) on titanium surfaces after 7 days of osteogenic induction

图6　钛表面不同硅烷偶联c(RGDfK)环肽各组细胞成骨诱导7 d后ALP活性

OHMPS组：P = 0.001），而OH组、OHCP组较NT组差异没有统计学意义（OH组：P = 0.173，OHCP组：P = 0.167）。

3　讨　论

RGD多肽是生物材料领域中研究最为广泛的功能性多肽之一，其在纤维粘连蛋白、层粘连蛋白等多种细胞外基质蛋白中检测出，且证实其能与细胞膜上多种整合素特异性识别，是人体内广泛存在并使用的肽序列[3,8-9]。在许多实验中，RGD多肽在促进多种细胞类型与不同材料的结合方面有效，目前RGD多肽在研究中的应用主要在于和多种活性物质共同作用、改善材料表面生物性能，也有研究将其用于靶向药物载体的制备。人工合成的环肽较线肽有更好的抗酶解能力和热稳定性，应用前景更广[3,10]。

对材料进行表面活化，运用偶联剂改性，进而负载多肽涂层是将多肽结合于钛表面的常用方法[4-6]。本研究中，首先按照文献[7]中的方法，对钛表面进行碱热处理，强碱对钛的腐蚀作用使得钛表面形成亚微米级三维网状结构的孔洞，可以提高金属表面润湿性。DAPI及鬼笔环肽染色后激光共聚焦显微镜下观察证实碱热处理也可以一定程度改善材料表面的细胞黏附。碱热处理还使钛表面负载了大量羟基，为利用硅烷偶联剂进一步进行表面改性提供了化学基础[11]。硅烷中的甲氧基或乙氧基水解后，可与碱热活化表面上的羟基发生缩聚反应，形成Ti-O-Si键，彼此之间在加热后也可形成Si-O-Si键，进一步稳定连接[12-14]。本实验中，可能由于碱热处理后部分孔隙较大，负载硅烷后呈现出部分孔隙被填满、部分孔隙未能填满的不完整的膜结构，这可能对硅烷涂层的强度有所影响，但碱热处理后的亚微米结构得以保留。考虑到c（RGDfK）仅是由五个氨基酸组成的环肽，分子量较小，其与硅烷结合后难以通过扫描电镜观察到其结构，填满孔隙的结构主要是聚合后的硅烷。其中，各组之间的孔隙填满的形态略有不同，这可能和不同末端基团的硅烷在钛表面的聚合方式差异有关。

硅烷的另一端为活性基团，可与c（RGDfK）反应。OHAP组中，主要依靠氨基与c（RGDfK）中羧基的静电相互作用以及碱热处理后的表面多孔形貌将其固定；MPTS组中，巯基与戊二醛的一侧醛基反应生成C-S键，另一侧醛基与c（RGDfK）的氨基反应生成席夫碱[5]；CPTES组中，来自CPTES有机官能团的氯原子是反应的亲电中心，c（RGDfK）中非结合部位的游离胺基是亲核基团，氯原子可以直接和氨基发生亲核取代反应[4]；而γ-MPS中的烯酰氧基可以和氨基发生氮杂Michael加成反应，乙烯基的双键打开，通过C-N键相连。

XPS结果证明c（RGDfK）结合于材料表面。本研究发现，MPTS、γ-MPS、CPTES均结合了较多的c（RGDfK），其生物学性能较处理前有所改善，OHMPS组负载c（RGDfK）环肽稍高于OHCP组及OHMPT组，但远未达到该组硅烷负载率的优势，可能是由于在温和环境下γ-MPS与c（RGDfK）反应不活泼。而APTES修饰后的钛表面虽然固定的c（RGDfK）不多，但对细胞黏附性能的改善较γ-MPS组反而更好。此前有学者认为，人工合成RGD多肽的促黏附效果与天然的有大量结合域蛋白相比较弱，在暴露于血清等有大量天然蛋白的溶液时，由于天然蛋白引发的信号传导，表面修饰的RGD多肽对细胞黏附的影响并不明显[3]。

本研究中，除OHCP组外，硅烷偶联c（RGDfK）处理后，细胞增殖和成骨分化活性均增强，OHMPT组、OHMPS组、OHAP组间没有显著差别。OHAP组虽然结合的c（RGDfK）较少，但其表面未反应的硅烷末端在溶液中可水解为带正电荷的NH_3^+，这有利于蛋白质的吸附，从而促进细胞黏附、增殖和成骨分化[15-17]。而OHCP组表面残留的硅烷末端水解后为带负电的Cl^-，这可以部分解释该组生物学性能不佳的问题。

基于以上分析，可以得出以下结论：MPTS、CPTES、γ-MPS三种硅烷能够作为偶联剂将c（RGDfK）环肽结合于钛表面，提供促进成骨细胞黏附、增殖和分化的作用，其中γ-MPS偶联c（RGDfK）环肽的效果最好，而MPTS、CPTES、γ-MPS连接c（RGDfK）环肽后具有相似的生物学性能。

【Author contributions】 Zhou QY designed the study, analyzed the data, wrote the article. Hong GY, Wu T assisted the performing of the experiments. Chen C, Xie HF designed the study and revised the article. All authors read and approved the final manuscript as submitted.

参考文献

[1] Chrcanovic BR, Kisch J, Albrektsson T, et al. A retrospective study on clinical and radiological outcomes of oral implants in patients followed up for a minimum of 20 years[J]. Clin Implant Dent Relat Res, 2018, 20(2): 199-207. doi: 10.1111/cid.12571.

[2] Smeets R, Stadlinger B, Schwarz F, et al. Impact of dental implant surface modifications on osseointegration[J]. Biomed Res Int, 2016: 6285620. doi: 10.1155/2016/6285620.

[3] Bellis SL. Advantages of RGD peptides for directing cell association with biomaterials[J]. Biomaterials, 2011, 32(18): 4205-4210. doi: 10.1016/j.biomaterials.2011.02.029.

[4] Chen X, Sevilla P, Aparicio C. Surface biofunctionalization by covalent co-immobilization of oligopeptides[J]. Colloids Surf B Biointerfaces, 2013,107: 189-197. doi: 10.1016/j.colsurfb.2013.02.005.

[5] Chen WC, Ko CL. Roughened titanium surfaces with silane and further RGD peptide modification *in vitro*[J]. Mater Sci Eng C Mater Biol Appl, 2013, 33(5): 2713-2722. doi: 10.1016/j.msec.2013.02.040.

[6] Paredes V, Salvagni E, Rodríguez-Castellon E, et al. Study on the use of 3-aminopropyltriethoxysilane and 3-chloropropyltriethoxysilane to surface biochemical modification of a novel low elastic modulus Ti-Nb-Hf alloy[J]. J Biomed Mater Res B Appl Biomater, 2015,103(3): 495-502. doi: 10.1002/jbm.b.33226.

[7] Yang Z, Xi Y, Bai J, et al. Covalent grafting of hyperbranched poly-L-lysine on Ti-based implants achieves dual functions of antibacteria and promoted osteointegration *in vivo*[J]. Biomaterials, 2021, 269: 120534. doi: 10.1016/j.biomaterials.2020.120534.

[8] Hersel U, Dahmen C, Kessler H. RGD modified polymers: biomaterials for stimulated cell adhesion and beyond[J]. Biomaterials, 2003, 24(24): 4385-4415. doi: 10.1016/s0142-9612(03)00343-0.

[9] Hautanen A, Gailit J, Mann DM, et al. Effects of modifications of the RGD sequence and its context on recognition by the fibronectin receptor[J]. J Biol Chem, 1989, 264(3): 1437-1442.

[10] Heller M, Kumar VV, Pabst A, et al. Osseous response on linear and cyclic RGD-peptides immobilized on titanium surfaces *in vitro* and *in vivo*[J]. J Biomed Mater Res A, 2018, 106(2): 419-427. doi: 10.1002/jbm.a.36255.

[11] Yu X, Xu R, Zhang Z, et al. Different cell and tissue behavior of micro-/nano-tubes and micro-/nano-nets topographies on selective laser melting titanium to enhance osseointegration[J]. Int J Nanomedicine, 2021, 16: 3329-3342. doi: 10.2147/IJN.S303770.

[12] Meroni D, Lo Presti L, Di Liberto G, et al. A close look at the structure of the TiO2-APTES interface in hybrid nanomaterials and its degradation pathway: an experimental and theoretical study [J]. J Phys Chem C Nanomater Interfaces, 2017, 121(1): 430-440. doi: 10.1021/acs.jpcc.6b10720.

[13] Ryu JJ, Park K, Kim H, et al. Effects of anodized titanium with Arg-Gly-Asp (RGD) peptide immobilized *via* chemical grafting or physical adsorption on bone cell adhesion and differentiation[J]. Int J Oral Maxillofac Implants, 2013, 28(4): 963-972. doi: 10.11607/jomi.2421.

[14] Senna PM, de Almeida BC, Mello-Machado RC, et al. Silane-coating strategy for titanium functionalization does not impair osteogenesis *in vivo*[J]. Materials (Basel), 2021, 14(7): 1814. doi: 10.3390/ma14071814.

[15] Hao L, Li T, Wang L, et al. Mechanistic insights into the adsorption and bioactivity of fibronectin on surfaces with varying chemistries by a combination of experimental strategies and molecular simulations[J]. Bioact Mater, 2021, 6(10): 3125 - 3135. doi: 10.1016/j.bioactmat.2021.02.021.

[16] Arima Y, Iwata H. Preferential adsorption of cell adhesive proteins from complex media on self-assembled monolayers and its effect on subsequent cell adhesion[J]. Acta Biomater, 2015, 26: 72-81. doi: 10.1016/j.actbio.2015.08.033.

[17] Lee MH, Boettiger D, Ducheyne P, et al. Self-assembled monolayers of omega-functional silanes: a platform for understanding cellular adhesion at the molecular level[M]. Leiden: Brill Academic Publishers, 2007: 82.

（编辑　张琳，管东华）

官网